Full-torus impurity transport simulation in multi-species impurity powder injection experiments in the Large Helical Device

Mamoru Shoji[1,2], Gakushi Kawamura[1,3], Roman Smirnov[4], Juri Romazanov[5], Andreas Kirschner[5], Yasunori Tanaka[6], Suguru Masuzaki[1,2], Tomoko Kawate[1,2], Erik P. Gilson[7], Robert Lunsford[7], Sebastijan Brezinsek[5], and Novimir A. Pablant[7]

[1]National Institute for Fusion Science, Japan
[2]The Graduate University for Advanced Studies, SOKENDAI, Japan
[3]National Institutes for Quantum Science and Technology, Japan
[4]University of California at San Diego, USA
[5]Forschungszentrum Jülich, Germany
[6]Kanazawa University, Japan
[7]Princeton Plasma Physics Laboratory, USA

Abstract

The toroidal distribution of the boron deposition on plasma facing components (PFCs) in boron powder injection by an impurity power dropper (IPD) was investigated by full-torus simulation using spectroscopic observations in a plasma density scan experiment. The images of the ablation of dropped boron powders observed in different plasma densities are consistent with the simulations which consider the size distribution of the boron powders. The analysis of the observed intensity profile of boron emission at a visible spectrometer by the simulation indicated that the boron deposition density on the PFCs installed far from the IPD is low for higher plasma densities compared to that for medium plasma density. These experimental results verify the previous simulations of the toroidal distribution of the boron deposition in both plasma densities.

Introduction

The Impurity Powder Dropper (IPD) has gotten attention as an alternative method for wall conditioning such as real-time boronization which can be performed without the interruption of plasma discharges and the magnetic field [1-4]. The real-time boronization is realized by continuously supplying boron powders during the plasma discharge. This method has advantages over conventional wall-conditioning method such as glow discharge cleaning using diborane (B_2H_6) gases [5]. In the Large Helical Device (LHD), an IPD has been installed in an upper port (2.5-U) to inject impurity powders into the plasma to investigate the effect of the boronization and impurity transport [6]. In the divertor configuration in LHD, real-time boronization using the IPD seems to be preferable from the viewpoint of forming boron deposition layers on the divertor plates installed in a closed divertor region.

The divertor plates do not directly face the main plasma, which means that the conventional glow discharge cleaning is not so effective in forming boron layers on the surface of the plates. One of the concerns of the boronization using the IPD is to achieve the toroidal uniformity of the distribution of the boron deposition on the plasma-facing components (PFCs) because the IPD is normally installed at one of the upper ports at only one toroidal position in the torus. Thus, the analysis of the full-torus impurity (boron) transport and the deposition profile on the PFCs is essential for making full use of the IPD for wall-conditioning. The impurity transport is strongly affected by the position and the spatial distribution of the impurity source in the plasma which is produced by the ablation of dropped boron powders.

In LHD, simulation using a dust transport code (DUSTT) [7-9] and a three-dimensional edge plasma code (EMC3-EIRENE) [10, 11] revealed that the position of the ablation position of the dropped impurity powders strongly depends on the plasma density [12]. The simulation showed that the boron powders dropped from the IPD must pass through an upper divertor leg before reaching the peripheral plasma (the ergodic layer) and indicated that the powders are evaporated by the heat load from the peripheral plasma, which results in the ablation of the boron powders. The simulation revealed that the ablation position changed toward the outboard side of the torus with the increase in the plasma density. This is because the trajectory of the dropped powders is deflected toward the outboard side by the effect of the plasma flow in the upper divertor leg [12]. The simulation using the three-dimensional plasma surface interaction (PSI) code (ERO2.0) [13, 14] predicted that the change in the ablation positions for higher plasma densities brought a localized distribution of the boron deposition on the PFCs adjacent to the IPD [15]. This is because of shorter connection lengths in the ergodic layer at the ablation positions in the outboard side. The magnetic field lines with the shorter connection lengths connect to the PFCs near the ablation positions.

To experimentally verify the prediction by the full-torus simulation, boron powder injection was performed with systematic scan of the plasma density. In the following sections, the observations of the ablation positions of the dropped boron powders in the experiment are analyzed by the simulation. The intensity profile of boron emission lines observed with a spectrometer array in the boron powder injection is investigated by the full torus simulation.

Analysis of the distribution of the ablation positions of the dropped boron powders

The atomic boron source profile is one of the essential parameters for the impurity transport simulation. The three-dimensional position and distribution of the boron source produced by the dropped boron powders in the plasma density scan experiment were calculated using DUSTT under fixed three-dimensional background plasma parameter profiles calculated by EMC3-EIRENE in which the plasma density just inside the Last Closed Flux Surface n_e^{LCFS}, the plasma heating power P^{LCFS}, perpendicular particle diffusion coefficient $D_\perp$ and electron/ion thermal diffusion coefficient

$\lambda_{i,e\perp}$ were set to reproduce the observed electron density and temperature profiles in the peripheral plasma. Figure 1 shows the time evolution of the representative plasma parameters in the density scan experiment in which the radial position of the magnetic axis in the major radius R_{ax} and the magnetic field B_t were 3.60 m and 2.75 Tesla, respectively. The line averaged plasma density was controlled to five different ones (1, 2, 3, 4, and 5×10^{19} m^{-3}) during the plasma discharges by feed-backed hydrogen gas fueling. In this experiment, boron powders with a nominal diameter of 150 μm were used. The boron powders dropped from the IPD reached the plasma at about 4 seconds and the injection was sustained up to 5 seconds. The plasma parameters were not significantly changed by the powder injection because of a small drop rate of about 1 mg/s in this experiment. While the radiation power, H_α and boron intensities, and the stored energy increased with the plasma density, the central electron temperature drops with the plasma density.

The position and distribution of the ablation of the boron powders were routinely observed with a Charge Coupled Device (CCD) camera installed in an upper port close to the IPD. Figure 2 displays the images of the ablation of the boron powders in three different plasma densities. The exposure time of the camera was set to 10 ms in the experiment. The camera detected several stripes of visible light during the powder injection especially for higher plasma densities. The boron powders are evaporated and release boron atoms with an energy of the evaporation temperature. The boron atoms are ionized and emit visible light by the interaction with the plasma. The boron ions move along the magnetic field lines, by which the ions produce the stripes of visible light along the field lines. Figure 2 shows that the main ablation area, where the stripes are concentrated with high brightness, was moved toward the outboard side of the torus with the increase in the plasma density, which also shows that the stripes disperse toward the outboard side for higher plasma densities.

The observed ablation images of the dropped boron powders were investigated using the DUSTT and EMC3-EIRENE. Figure 3 displays a perspective view of the three-dimensional model of the vacuum vessel and the peripheral plasma in R_{ax}=3.60 m for half of one helical section (18° in toroidal direction) which was made for calculating the trajectories of dropped boron powders and the ablation positions. In this analysis, the boron powders were dropped by gravity from the initial position underneath a tube for guiding the powders to the peripheral plasma. The downward velocity at the initial position was set to 5 m/s which corresponds to the velocity in the case where a boron powder is dropped from the actual position of the IPD locating outside of the figure. From the loss rate of the mass of the powders along the trajectories, the spatial distribution of the production rate of boron atoms evaporated from the powders was calculated by DUSTT. The size distribution of the boron powders was recently revealed by microscopic analysis, showing an average major axis length of the powders of about 107 μm with a half-value width of 28 μm [16]. These values are newly implemented in DUSTT by dividing the size distribution into more than one hundred groups of different sized powders. Figure 4 presents perspective views showing the distribution of the production rate of boron

atoms in the peripheral plasma for three different plasma densities (n_e^{LCFS}=1, 3, 5×10^{19} m^{-3}), in which the production rate is expressed as colored spheres. The framework of the figures corresponds to the area indicated as the broken gray square in Figure 3. The main ablation area of the boron powders is indicated as a group of red spheres, which exhibits that the position of the main ablation area moves toward the outboard side with the increase in the plasma density and the distribution disperse to the outboard side for higher plasma densities. The change in the position of the main ablation area can be explained by the deflection of the trajectories of the dropped boron powders due to the effect of the plasma flow in the upper divertor leg. The plasma flow is more influential in dispersing smaller-sized powders to the outboard side, which is consistent with the observed images of the ablation positions of the dropped boron powders shown in Figure 2.

Full torus simulation of impurity transport in boron powder injection experiments with plasma density scan

Full torus impurity transport simulation in the plasma density scan experiment was performed in order to investigate spectroscopic observations. Figure 5 shows the time trend of the line-integrated intensity profile of two boron emission lines (BI and BII) at a plasma discharge with boron powder injection for a high plasma density of n_e~5×10^{19} m^{-3}, which was observed with a vertical visible spectrometer array installed in an outer port (10-O) [17, 18]. The observations show an increase in the intensity of the boron emission during the powder injection. In the left side in this figure, a poloidal cross-section of the vacuum vessel, the divertor plates and a LHD plasma on the poloidal surface along the Line Of Sight (LOS) of the spectrometer is illustrated. The cross-section of the profile of the radiation power density by B^+ calculated by EMC3-EIRENE is also shown, in which the sputtering rate of boron by the background hydrogen plasma was assumed to be 0.01. The observed intensity at the channels having LOS viewing the front of the divertor plates installed in the inboard side was higher than that at the other channels, showing the sputtering of boron on the divertor plates. Figure 6 (a) and (b) present the intensity profile of the two boron emission lines before and during the powder injection in the plasma density scan experiment, respectively. The exposure time of the spectrometer was set to 50 ms in the experiment. The figures show that the intensity was small in lower plasma densities, and the intensity at around channels 25 and 35 was high for higher plasma densities regardless of the powder injection. It has been found that the high intensity at around channel 35 viewing a roof-shaped dome in the closed divertor region cannot be reproduced by the simulation as shown in the left figure in Figure 5. One of the possible candidates for explaining the high intensity could be due to PSIs on the surface of the dome because the distance between the dome and the peripheral plasma is short (~10 mm). The PSIs on the dome cannot be exactly taken into account in the simulation, which can disturb the detailed analysis of the impurity transport in the boron powder injection. For this reason, the perturbation method was applied to the analysis by subtracting the

intensity profile before the powder injection from that during the injection, which derives only the increment of the intensity induced by the boron powder injection. Figure 6 (c) shows the extracted intensity profile which exhibits successful subtraction of the intensity at around channel 35. The figure shows the observable peak at around channel 25 for a medium plasma density (n_e~3×10^{19} m^{-3}). It should be noted that the peak gradually decreases with the increase in the plasma density.

The subtracted intensity profile of the two boron emission lines was investigated by a full-torus simulation using ERO2.0. Figure 7 (a) illustrates the full-torus model for the simulation in which calculations by EMC3-EIRENE were used as the three-dimensional background plasma parameter profiles. The calculations by DUSTT were adopted as the distributions of the atomic boron source originating from the dropped boron powders. The initial position underneath the IPD and the LOS of the visible spectrometer array is indicated as a yellow sphere and green lines, respectively. It should be noticed that the position of the spectrometer array is toroidally far from the IPD. In the ERO2.0 simulation, it was assumed that the material of the plasma-facing side of the divertor plates was boron and no boron sputtering by the background hydrogen plasma (only self-sputtering of boron originating from the dropped boron powders was considered). The material of the other part of the PFCs was assumed to be carbon which is one of the dominant materials of in-vessel components in LHD. Figure 7 (b) gives the simulation of the full-torus density profile of neutral boron atoms evaporated from the powders for a medium plasma density (n_e=3×10^{19} m^{-3}), in which the boron atoms are localized near the toroidal section where the IPD is installed. In this figure, the poloidal cross-sections of the boron density profile are displayed at the toroidal positions where the shape of the plasma is horizontally and vertically elongated. Figure 7 (c-f) exhibit the simulations of the density profile of boron ions with different charge states, showing that the boron ions toroidally diffused with the charge state. The density of singly and doubly charged boron ions (B^+ and B^{++}) was localized in the divertor region in the inboard side such as shown in Figure 5. Using the three-dimensional profile of the background plasma parameters and the calculated boron atom/ion densities, the profile of the radiation power density of the two boron emission lines was derived using an atomic-molecular database provided by ADAS [19]. By integrating the radiation power density along the LOS of the channels of the spectrometer, the intensity profile of the boron emission lines was obtained. Figure 8 displays the simulations of the intensity profile for the high and medium plasma densities, in which the peak of the intensity for the high plasma density is about one-third of that for the medium plasma density in both boron emission lines. Comparison of the simulations with the observations in Figure 6 (c) for the high and medium plasma densities revealed that the observed ratio of the peak of the intensity in the high plasma density on that in the medium plasma density is much smaller than the simulation. This discrepancy between the simulations and the observations indicates a lower sputtering rate of boron on the divertor plates in the high plasma density in the experiment, which can be due to the lower density of boron deposited on the divertor plates in the high plasma density. The previous full-torus

simulation using ERO2.0 predicted a toroidally localized boron deposition near the IPD in the high plasma density, and more uniform boron deposition in the medium plasma density [15]. The observed lower sputtering rate in the high plasma density is consistent with the previous ERO2.0 simulations which indicated a lower density of boron deposition on the divertor plates in the LOS of the spectrometer installed far from the IPD. The reason for the different toroidal distribution of the boron density in the two plasma densities is the change of the ablation positions of the dropped boron powders in the peripheral plasma where the connection length becomes shorter as the position changes to the outboard side.

Summary

The toroidal distribution of the boron deposition profile on the PFCs induced by boron powder injection in a plasma density scan experiment was investigated by the full-torus simulation. The simulation showed that the main ablation area of the dropped boron powders changed toward outboard side of the torus with the increase in the plasma density and the distribution of the ablation positions dispersed toward the outboard side for higher plasma densities, which are consistent with the observed images of the ablation of dropped boron powders. The intensity profiles of two boron emission lines (BI and BII) before and during the boron powder injection were observed with a visible spectrometer array. By subtracting the intensity profile before the powder injection from that during the injection, the incremental change caused by the boron powder injection was successfully extracted. The extracted intensity profiles in the plasma density scan experiment were investigated by ERO2.0 using a full torus model, which revealed that the observed ratio of the peak of the intensity for the medium plasma density on that for the high plasma density is different from the simulation. This discrepancy indicates a lower density of boron deposited on the divertor plates in the inboard side for the high plasma density. The toroidal position of the divertor plates in the LOS of the spectrometer array is far from the IPD. Thus, this result experimentally verifies the previous full-torus simulation showing a localized boron deposition in the toroidal section adjacent to the IPD for the high plasma density.

Acknowledgements

This work was performed under the auspices of the NIFS Collaboration Research program (NIFS20KIST004). One of the authors (M. S.) would like to thank Y. Feng for permission to use EMC3-EIRENE. He is also grateful for the computational resources of the plasma simulator in NIFS. This work is supported by a JSPS KAKENHI Grant Number 21K18620. This work is also supported by the U.S. Department Of Energy under Contract No. DE-AC02-09CH11466 with Princeton University.

References

[1] A. Nagy et al., Rev. Sci. Instrum. **89** (2018) 10K121.

[2] R. Lunsford et al., Nucl. Fusion **59** (2019) 126034.

[3] A. Bortolon et al., Nuclear Fusion **60** (2020) 126010.

[4] R. Lunsford et al., Nucl. Fusion **62** (2022) 086021.

[5] K. Nishimura et al., J. Nucl. Mater. **337** (2005) 431.

[6] N. Federico et al., Nuclear Materials and Energy **25** (2020) 10842.

[7] A. Y. Pigarov et al., Phys. Plasmas **12** (2005) 122508.

[8] R. D. Smirnov et al., Plasma Phys. Controlled Fusion 49 (2007) 347.

[9] Y. Tanaka et al., J. Nucl. Mater, **415** (2011) S1106.

[10] Y. Feng et al., Plasma Phys. Controlled Fusion **44** (2002) 611.

[11] G. Kawamura et al., Contrib. Plasma Phys. **54** (2014) 437.

[12] M. Shoji et al., Contrib. Plasma Phys. **60** (2020) e201900101.

[13] J. Romazanov et al., Nucl. Mater. Energy **18** (2019) 331.

[14] J. Romazanov et al., Nucl. Fusion **62** (2022) 036011.

[15] M. Shoji et al, Nuclear Materials and Energy **25** (2020) 100853.

[16] S. Sawford et al., 65th Annual Meeting of the APS (2023), CP11.00123.

[17] M. Goto et al., Fusion Science and Technology **58** (2010), 394.

[18] T. Kawate et al., Nucl. Fusion **62** (2022) 126052.

[19] The ADAS User Manual (version 2.6) https://www.adas.ac.uk/ (2004).

Figures

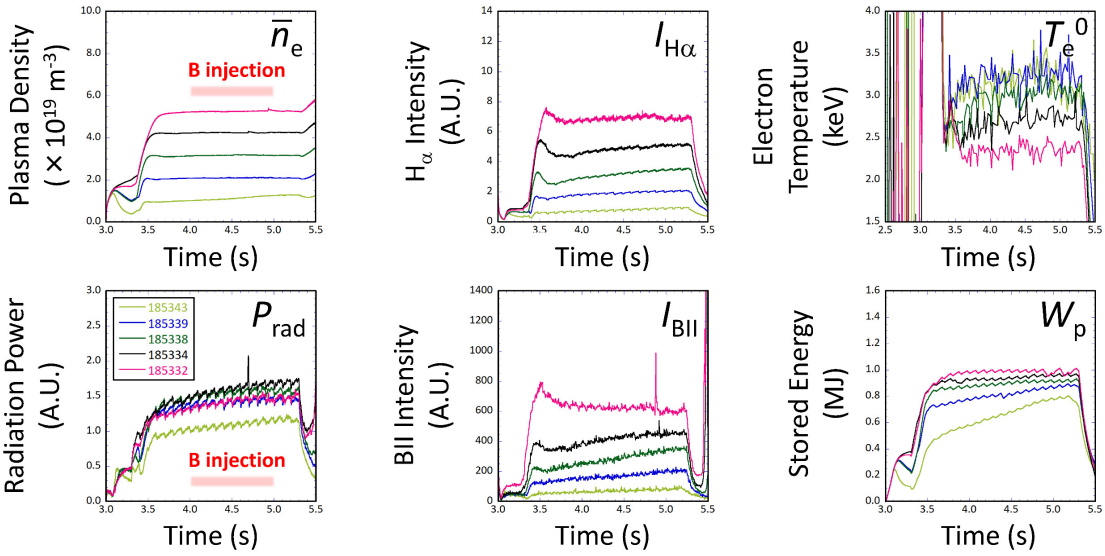

Fig. 1.

The time trend of representative plasma parameters (average plasma density, H_α intensity, central electron temperature, radiation power, BII intensity, and stored energy) in the plasma density scan experiment with boron powder injection for R_{ax}=3.60 m.

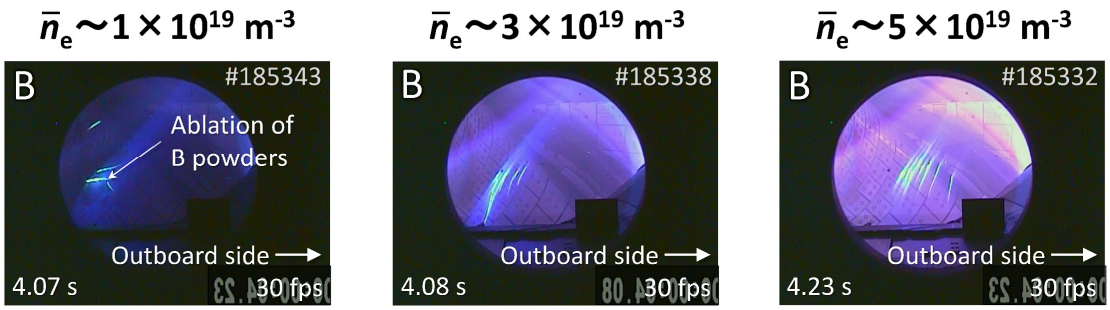

Fig. 2.

The images of the ablation of dropped boron powders in three different plasma densities, which were observed with a CCD camera installed in an upper port next to the position of the IPD.

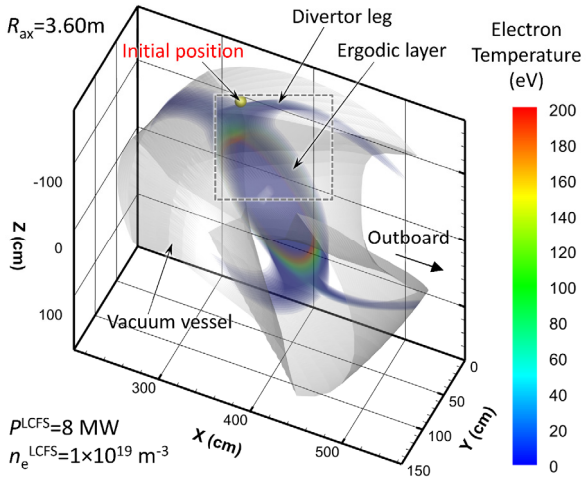

Fig. 3.

A perspective view of a three-dimensional model of the vacuum vessel and the peripheral plasma for half of one helical section (18^o in toroidal direction) to calculate the trajectories and ablation positions of dropped boron powders. The poloidal cross-sections of the electron temperature profile in the plasma for P^{LCFS}=8 MW and n_e^{LCFS}=1×10^{19} m^{-3} are illustrated inside the vacuum vessel.

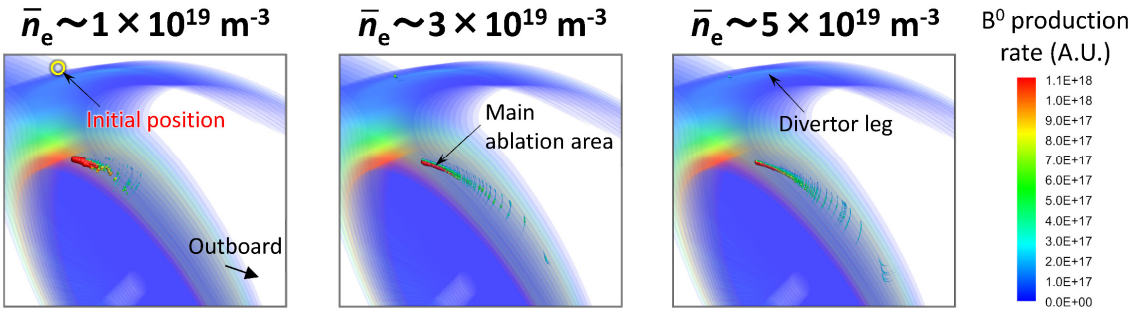

Fig. 4.

The calculations of the distribution of the ablation positions of the dropped boron powders in the peripheral plasma for three different plasma densities. The production rate of boron atoms originating from dropped boron powders is indicated as colored spheres.

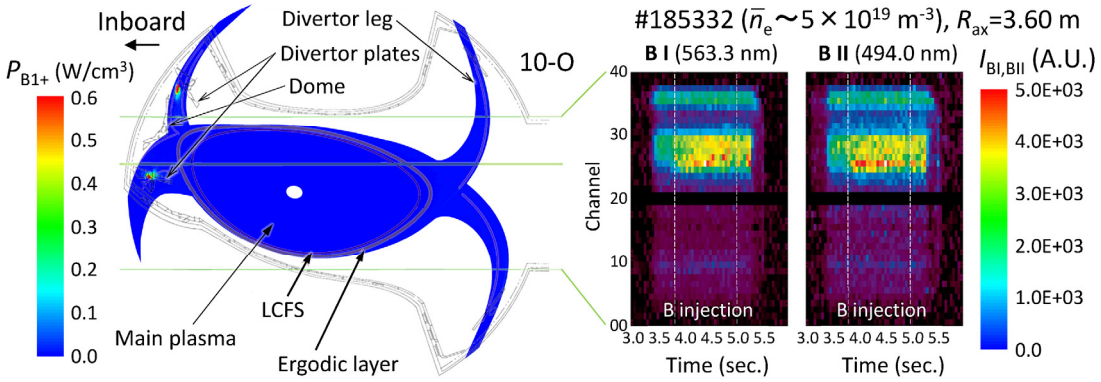

Fig. 5.

The observed time trend of the line-integrated intensity of two boron emission lines (BI and BII) for a high average plasma density of 5×10^{19} m^{-3} in the plasma density scan experiment (right figures). The poloidal cross-section of the vacuum vessel, the divertor plates, and the plasma along the LOS of the visible spectrometer array is illustrated in the left figure. The cross-section of the profile of the radiation power density by B^+ calculated by EMC3-EIRENE for the high-plasma density is also shown in this figure.

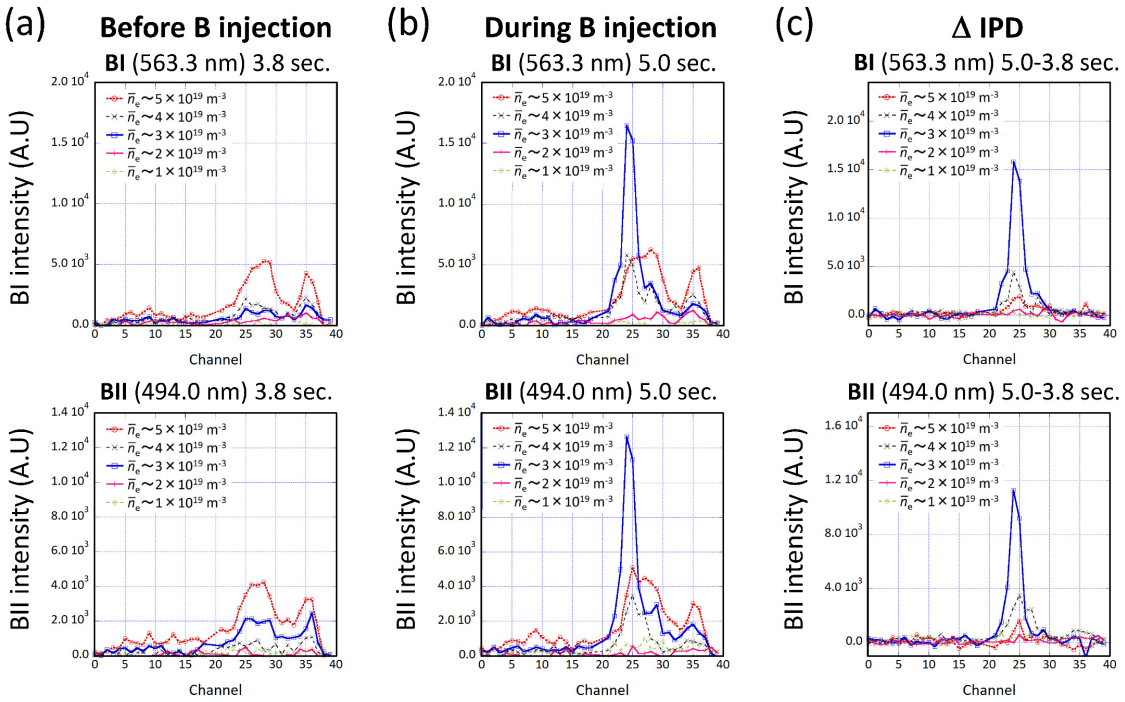

Fig. 6.

The observations of the line-integrated intensity profile of the two boron emission lines (BI and BII) before (a) and during the boron powder injection (b) in the plasma density scan experiment. The extracted increment of the intensity profile by the boron powder injection in this experiment is shown in figure (c).

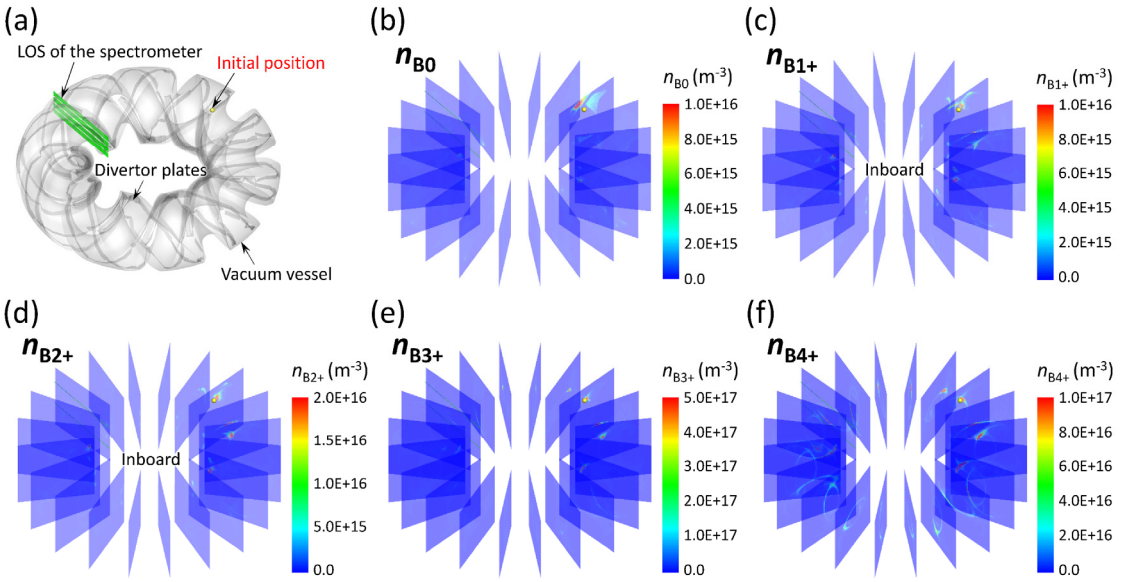

Fig. 7.

(a) A perspective view of the full-torus model of the vacuum vessel and the divertor components for the simulation. The simulation of the full-torus density profile of neutral boron atoms (b) and boron ions with different charge states (c-f) originating from the dropped boron powders. In figures (b-f), the poloidal cross-sections of the profiles are displayed at the toroidal positions where the shape of the LHD plasma is horizontally and vertically elongated.

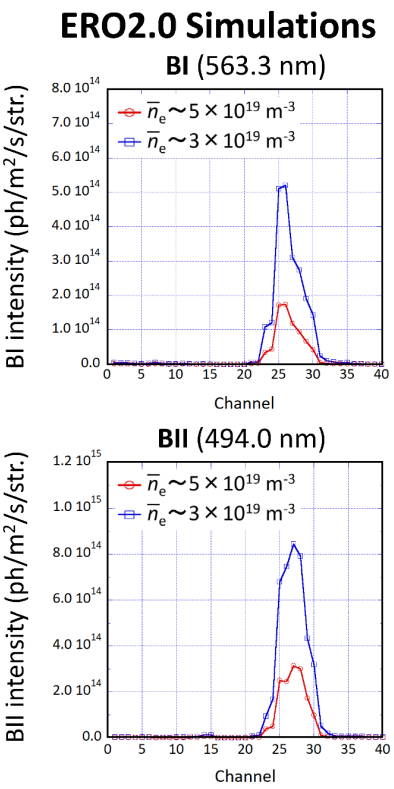

Fig. 8.

Simulations of the line-integrated intensity profile of the boron emission lines (BI and BII) along the LOS of the visible spectrometer array for high and medium plasma densities.